Check for updates

A Robust Triboelectric Nanogenerator Resistant to Humidity and Temperature in Ambient Environment

Smitha Ankanahalli Shankaregowda, Chandrashekar Bananakere Nanjegowda, Shirong Guan, Jiaqi Huang, Jingyi Li, Rumana Farheen Sagade Muktar Ahmed, Krishnaveni Sannathammegowda,* Anandraju Madaveeranahally Boregowda, Fei Wang,* and Chun Cheng*

Triboelectric nanogenerator (TENG) is an energy harvesting technology from widespread mechanical energy based on the combined effects of triboelectrification and electrostatic induction. TENG devices are promising to be integrated into human daily life and their stability in the ambient environment is quite crucial to guarantee robust output. This requirement is increasing exponentially for powering various wearable/portable electronics and still remains as a challenge. Herein, contact and separation mode-based, humidity- and temperature-resistant TENG (HT-TENG) is fabricated utilizing ethylene vinyl acetate and polytetrafluoroethylene tape as frictional layers. By harvesting biomechanical energy, the device could generate peak-to-peak open circuit voltage of ≈210 V and short-circuit current of ≈12.85 µA, respectively. The as-fabricated device is tolerant to fluctuating relative humidity ranging from 10% to 60% and temperature ranging from 10 to 60 °C. Further, the device is shown to charge 22 and 47 µF commercial capacitors to 3 V using rectifier bridges, glowing light-emitting diodes, powering digital wrist watches, and a calculator. Thus HT-TENG as an efficient power source reliably operates not only in typical conditions, but also in desert and frigid environments, thereby extending the applicability and commercialization of the device in the global environments.

1. Introduction

The triboelectric nanogenerator (TENG) is a relatively new technology that can collect energy from nearly all dynamical motions in the environment and transform it into electricity as a power source.[1] TENG's performance boosting and reliability have been studied by the research community since its inception.[2] The surface charge densities of the selected materials, as well as selecting a suitable material from the triboelectric series, are critical factors in determining the device output.[3] However, stability is also pivotal, when TENG-based energy harvesting device has to work in ambient environments, particularly at extreme temperature, high/low humidity, or corrosive conditions. Humidity degrades the stability of TENG by creating a water barrier on the surface of the frictional layer, which may hamper charge transfer or deteriorate the induced charges, preventing their full-scale commercialization for everyday use.[4] Furthermore, as the temperature increases, the dielectric constant of the polymer changes, resulting in a difference in the polymer's ability to lose or gain electrons,[5]

S. A. Shankaregowda, S. Guan, J. Huang, J. Li, C. Cheng
Department of Materials Science and Engineering
Southern University of Science and Technology (SUSTech)
Shenzhen 518055, P. R. China
E-mail: chengc@sustech.edu.cn

S. A. Shankaregowda, A. M. Boregowda
Department of Electronics and Communication Engineering
BGS institute of Technology
Adichunchanagiri University
Karnataka 571448, India

C. B. Nanjegowda
Department of Chemistry
Sri Adichunchanagiri First Grade College
University of Mysore
Channarayapatna, Karnataka 573116, India

R. F. S. M. Ahmed, K. Sannathammegowda
Department of Studies in Physics
University of Mysore
Mysuru, Karnataka 570006, India
E-mail: sk@physics.uni-mysore.ac.in

F. Wang
School of Microelectronics
Southern University of Science and Technology
Shenzhen 518055, P. R. China
E-mail: wangf@sustech.edu.cn

C. Cheng
Guangdong Provincial Key Laboratory of Energy Materials for Electric Power
Southern University of Science and Technology (SUSTech)
Shenzhen 518055, China

affecting the TENG's efficiency. The effect of varying humidity environments and temperature on the electrical output of TENG is very significant and interesting to investigate, particularly when self-driven electronics powered by TENG are used in certain severe conditions such as rainy days, sweating skin, cold areas, and desert regions.

Several attempts have been made to investigate the stability and effect of the electrical performance of TENG on varying humidity and temperature. Nguyen et al.[4b] reported that, when humidity increases from 10% to 90%, the charges generated on as-fabricated TENG decrease by about 25%. Guo et al.,[6] fabricated a humidity sensor-based TENG with polytetrafluoroethylene (PTFE) and fluorine-doped tin oxide glass as frictional layers and traced the voltage and current values by changing relative humidity (RH) at the fixed airflow rate of 25 L m^{-1}. With the increase in RH from 20% to 100%, the output current and voltage decreased by about 8.2 times and 2 times, respectively. Even though, the above investigations are cutting–edge research, efforts have been made only toward improving the output performance and to avoid the decay in the output with increasing %RH, without focusing on the stability of the device. Generally, the temperature in our ambient environment fluctuates with time. The TENG should be stable and durable to work in such fluctuating temperature conditions. Wen et al.[5b] studied the influence of temperature on the output performance of TENG composed of PTFE film and aluminum (Al) foil as contact materials. The output voltage and current were measured from 300 to 500 K and from 77 to 300 K, respectively. At around 260 K, output obtained was maximum and degrades at both higher and lower temperature. Similarly, Xia et al.[5a] demonstrated a TENG as a temperature sensor composed of PTFE and polyvinylidene fluoride as contact polymers and a copper (Cu) foil as electrode. The output voltage increased linearly with increasing temperature from 10 to 90 °C. Lu et al.,[5c] showed that the electrical performance of the TENG decreases as the temperature increases from 20 to 150 °C. Still much research is required toward improving the stability and electrical performance of the device to work in ambient environment.

To overcome this problem, designing a TENG with better performance which is stable under varying humidity and temperatures without altering or damaging its physical and electrical properties is highly desirable. TENG devices built with contact and separation mode also have triboactive layers that are either a dielectric–metal pair or a dielectric–dielectric pair.[3a] When the metal electrode of a dielectric–metal pair is exposed to the atmosphere, it corrodes, which in turn affects the performance of the TENG.[7] The dielectric–dielectric combination, on the other hand, can prevent the formation of a corrosive oxide layer and retain the device longevity. Hence the TENG with dielectric–dielectric pair is favorable for fabricating humidity and temperature resistance. As triboelectric materials play a vital role in regulating every aspect related to performance enhancement of TENG,[8] triboelectric series provides a brief idea in selecting the best candidate to be utilized in fabricating TENG.[9] Ethylene vinyl acetate (EVA) and PTFE have been commonly used as one of the triboelectric polymers in previously reported TENGs.[2a, d,10] Both the polymers possess robust features such as flexibility,[11] mechanical durability,[12] chemical resistance,[13] crack resistance,[14] and provides protection against varying weather

conditions upon exposure.[15] The water absorption rate of EVA and PTFE ranges from 0.005 to 0.13% and 0.005 to 0.01% weight in 24 h, indicating hydrophobicity in both the polymers.[16] Hence, suitable material is revealed for some applications which can avoid or overcome moisture-related failures. The hottest temperature recorded till date on planet Earth is 56.7 °C;[17] interestingly, the melting point of EVA is 120 °C and PTFE is 327 °C, below which the polymer is thermally stable. Furthermore, experiments have proved that EVA films stored in the dark at ambient temperature have no evidence of degradation for 6 years.[18] Similarly, PTFE possesses high capability to store charges for hundreds of years.[19] Thus, the combination of EVA and PTFE films can be used prosperously as active triboelectric layers in assembling TENG device suitable for ambient environment.

Herein, in this article, we propose a humidity and temperature-resistant TENG (HT-TENG), configured with contact and separation mode. The lower layer of HT-TENG comprises the EVA film as tribopositive material and upper layer consists of PTFE film as tribonegative material, Al as electrode, and polyethylene terephthalate (PET) as a supporting substrate on both the layers. The device generated maximum peak-to-peak open-circuit voltage (V_{OC}) and maximum peak-to-peak short-circuit current (I_{SC}) of ≈210 V and ≈12.85 µA, respectively, with a maximum power of 6.16 mW at a load resistance of 45 MΩ. The stability of HT-TENG was analyzed under various RH and temperature conditions ranging from 10 to 60%RH and 10 to 60 °C, respectively. The device produced a constant output voltage and current for varied RH and temperature. Furthermore, the device was used for charging commercial capacitors with capacitance 22 and 47 µF up to 3 V using hand-tapping energy, glowing light-emitting diodes (LEDs), powering a digital wrist watch, and a calculator. The reported work provides an efficient pathway for developing flexible devices working in ambient environment for self-powered systems.

2. Experimental Section

2.1. Preparation of 5% EVA Solution

5 g of EVA crystals (18% vinyl acetate and 72% ethylene, Aladdin Industrial Corporation, Shanghai) and 100 mL of cyclohexane were poured into a 150 mL beaker. For dissolving EVA crystals in cyclohexane, the mixture was heated on a hot plate with a magnetic stirrer at 70 °C for 24 h, forming 5% EVA solution, as schematically illustrated in **Figure 1**a.

2.2. Fabrication of HT-TENG

The as-obtained 5% EVA solution was spin coated on Al/PET substrate with the dimension 40 × 40 mm^2 as lower layer, and commercially available thermally resistant PTFE tape was attached to Al/PET with the dimension 40 × 40 mm^2 as the upper layer of the TENG. Both the layers were bent to form an arch shape for easy and better contact and separation. Here, EVA thin film was a tribopositive material, PTFE film was a tribonegative material, Al acted as electrode, and PET as supporting substrate for both the layers.
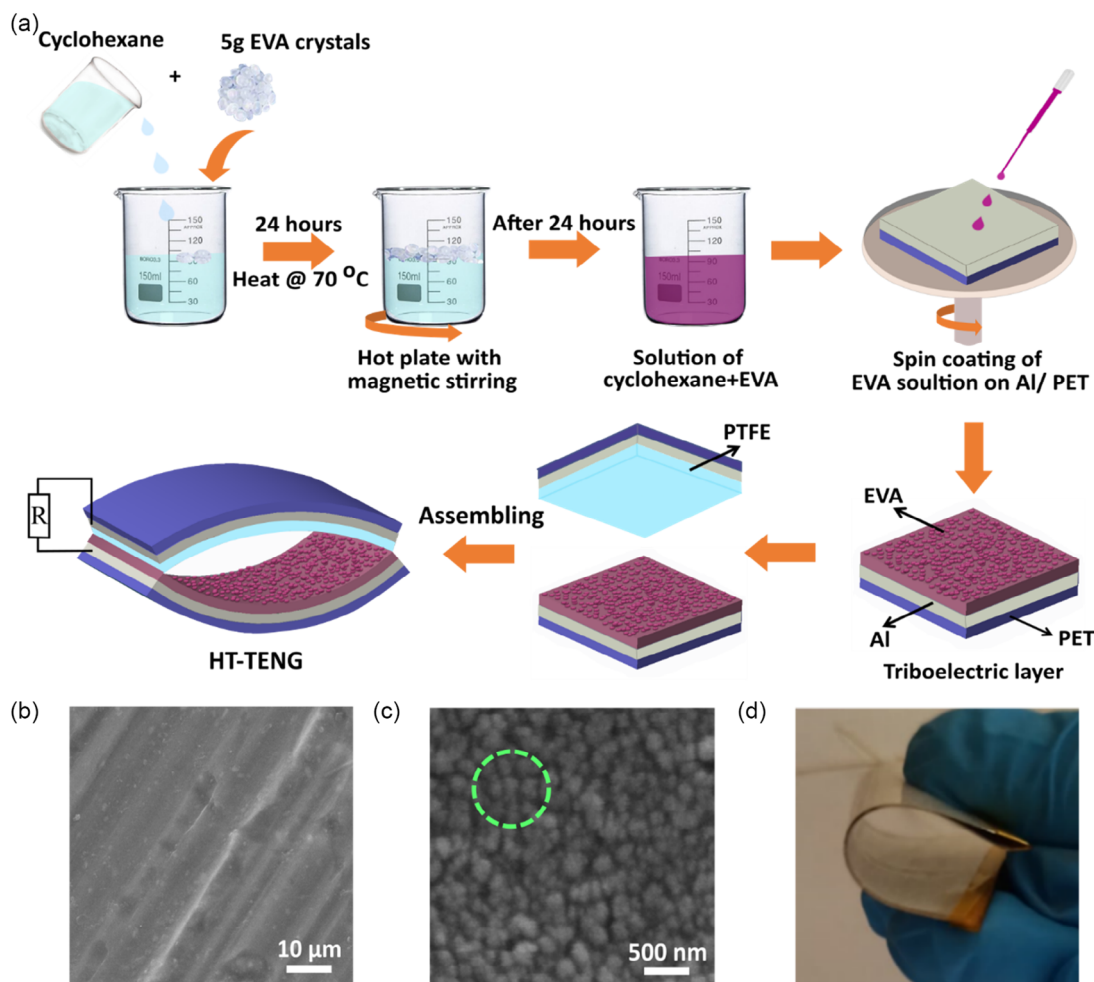
Figure 1. Fabrication of HT-TENG and its surface characterizations. a) Schematic illustration of fabricating HT-TENG device. b) The SEM image of bare Al surface. c) The SEM image of EVA thin film coated on Al showing bumpy structure. d) Photograph of flexible HT-TENG.

2.3. COMSOL Simulations

Electrostatic simulations were performed for the as-fabricated HT-TENG using COMSOL Multiphysics 5.5 software to obtain qualitative understanding of the working mechanism. The finite-element method (FEM) simulations were performed between the surfaces of PTFE and EVA with the dimension 40×40 mm^2. The thicknesses of PTFE and EVA were 0.06 and 0.01 mm with the surface charge density on both the layers as -10 and $+10$ μC m^{-2} respectively.

2.4. Characterization and Electrical Measurement

The surface characterization was done with scanning electron microscope (SEM) (ZEISS-Merlin, Oberkochen, Germany). The contact angle measurement was performed using a contact angle tester (AST products Inc., Billerica, USA). The short-circuit current and open-circuit voltage were measured by the Stanford low-noise current preamplifier (Model SR570, Stanford research system, Sunnyvale, CA, USA) and electrometer (Keithley 6514

System Electrometer, Beaverton, OR, USA), respectively. A custom-made glove box was used to measure humidity and temperature. The output voltage signal with varying %RH and temperature was measured using a digital oscilloscope (RIGOL DS1054Z 50 MHZ) and Stanford low-noise current preamplifier (Model SR570, Stanford research system, Sunnyvale, CA, USA) respectively with 10 MΩ load resistance.

3. Results and Discussion

3.1. Surface Characterizations of the HT-TENG

The complete fabrication process of HT-TENG is schematically illustrated in Figure 1a. First, 5 g of EVA crystals is poured into 100 mL of cyclohexane. To dissolve completely in cyclohexane, EVA crystals require a constant supply of heat and stirring. To obtain a 5% EVA solution, the mixture is heated at 70 °C for 24 h on a hot plate under continuous stirring using a magnetic stirrer. The obtained 5% EVA solution is spin coated for 30 s at 400 rpm on an Al/PET substrate. To ensure a uniform thin layer

of EVA film on Al/PET substrate, the spin-coating process is repeated with 1000 rpm for 60 s and dried at room temperature for 24 h. Surface roughness in the form of ridges and furrows of Al, as seen in the SEM image in Figure 1b, helps to hold the EVA firmly. During the preparation of 5% EVA solution, EVA crystals are heated in cyclohexane; as the temperature increases, EVA decomposes by liberating gases such as CO_2 and N_2,[20] which include short-chain (C2 to C4) aliphatic hydrocarbons and halogenated (C1 to C4) aliphatic hydrocarbons.[21] The liberated CO_2 acts as physical foaming agent for the production of polymeric foams/bumpy/bubble structures, as shown in the SEM image in Figure 1c and S1, Supporting Information. The presence of the micro-/nanoscale bumpy structure increases the surface area of the polymer,[22] which provides greater friction during the contact and separation process of HT-TENG, resulting in enhanced surface charge density and overall performance of the device. The real-time image of HT-TENG is as shown in Figure 1d, showing its flexibility.
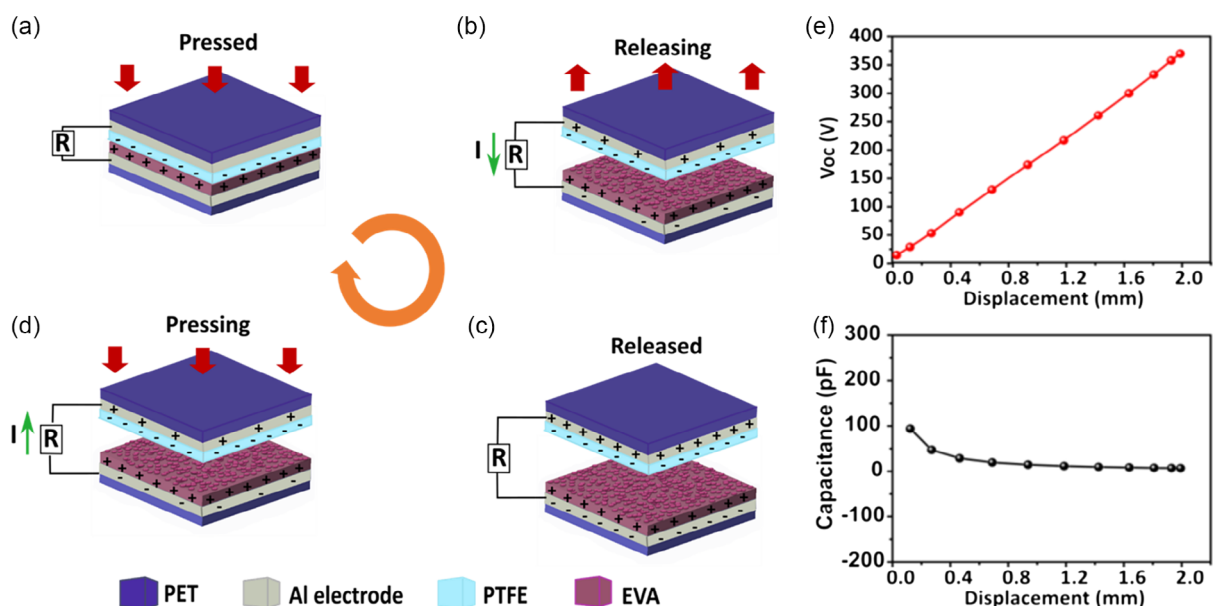
3.2. Working Mechanism of HT-TENG

The electricity generation process of the contact and separation based HT-TENG in one complete cycle is illustrated in **Figure 2**. Initially, both PTFE and EVA films are made in contact with each other by applying external force, and opposite charges are induced on the respective surfaces based on the polarity, as shown in Figure 2a. As PTFE is a tribonegative polymer, it will induce negative charges and EVA with positive charges, as it is a tribopositive polymer. When the external force is released, the electric potential is developed between the back electrodes (Al), driving electrons to flow through external circuit (Figure 2b). Again, when the device is brought into equilibrium,

charges does not flow (Figure 2c). Subsequently, when the upper layer is pressed, an electric potential difference with reversed polarity is produced, resulting in the electrons to flow in a reversed direction (Figure 2d), which leads to alternating output current during contact and separation of HT-TENG.

The effects of separation distance (x) between PTFE and EVA on the electric potential distribution and capacitance are shown in Figure 2e,f. The potential distribution between the two Al electrodes for separation distances from $x = 0$ mm to $x_{max} = 2$ mm under open-circuit voltage are simulated using COMSOL Multiphysics. Figure 2e shows that, when x increases from 0 mm to its maximum value, the V_{oc} also increases and reaches up to $\approx$370 V. Further, by varying separation distance, the electrical potential also increases and reaches up to 10^3 V for 10 mm separation distance, as shown in Figure S2, Supporting Information (Note S2 in Supporting Information). The capacitance of the device ($C(x)$) as a function of displacement is plotted as shown in Figure 2f. Initially at separation distance of 0.123 mm, the capacitance is $\approx$94 pF; as the separation distance increases, $C(x)$ of the device decreases up to $\approx$7 pF and reaches saturation. For lower displacement of triboelectric layers, the bigger the capacitance of the device, the higher the higher charge density.

3.3. Electrical Output Performance of HT-TENG

The output performance of HT-TENG with the active contact area of 40×40 mm^2 is evaluated using continuous hand-tapping mechanical energy. During the periodic contact and separation of PTFE film and EVA film, device generated a maximum peak-to-peak V_{oc} and I_{sc} of about $\approx$210 V and $\approx$12.85 μA, respectively, as shown in **Figure 3**a,b. The maximum peak-to-peak

Figure 2. Schematic illustration of the working mechanism of HT-TENG. a) Initially, the upper PTFE is fully in contact with the EVA surface. b) The release of the external force causes electrons to flow across Al electrodes through an external circuit. c) The equilibrium state. d) Electrons flow back due to the reapplied external force. The FEM simulated values of e) open-circuit voltage and f) capacitance of the device for various displacements ranging from 0 to 2 mm.
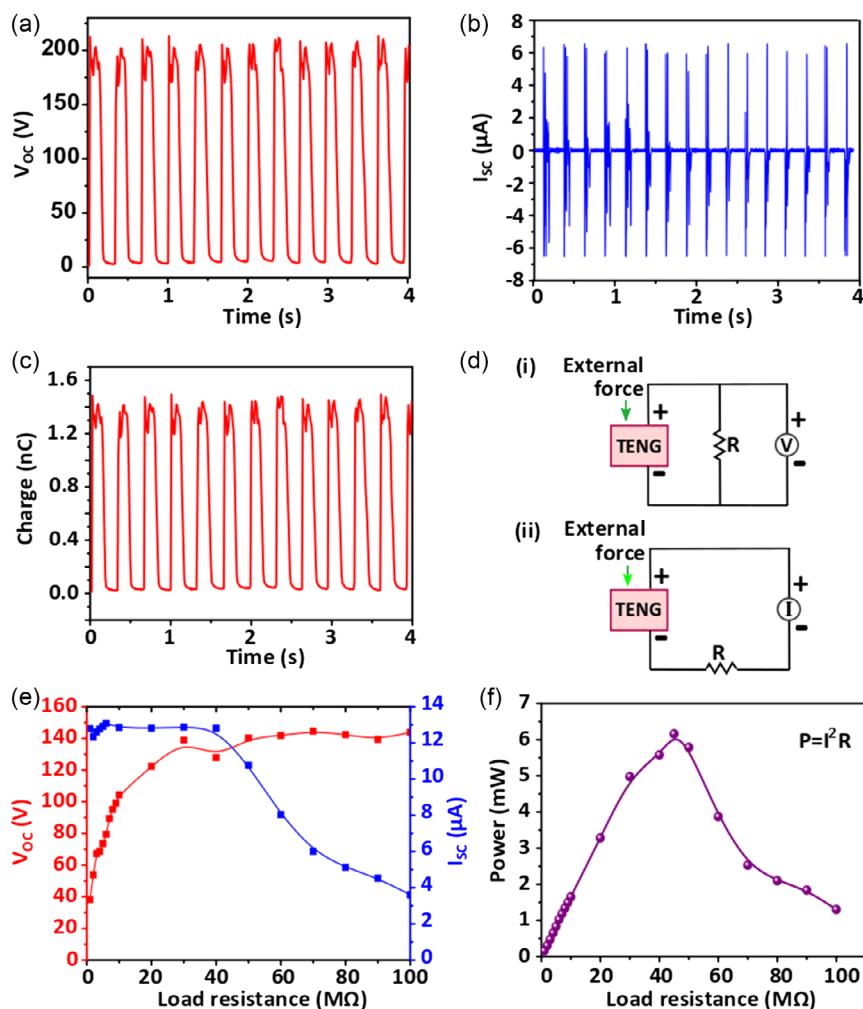
Figure 3. Electrical characterization of HT-TENG. Plot of a) open-circuit voltage. b) Short-circuit current. c) Charges transferred. d) Circuit diagram for measuring (i) voltage and (ii) current. e) Open-circuit voltage and short-circuit current versus external load resistance. f) Output power for various load resistances.

charge transfer quantity obtained is about ≈1.47 nC, as shown in Figure 3c, and the detailed parameters used in calculations are given in Table S1 and Note S2, Supporting Information. It signifies that ≈1.47 nC of charges are transferred from one electrode to other one at a maximum separation distance of 2 mm.

We have investigated the output voltage and current behavior of HT-TENG by varying load resistance from 10 to 100 MΩ. The circuit diagram for measuring the output voltage (Figure 3d-i) and current (Figure 3d-ii) across the load resistance is as shown in Figure 3d. It was found that the voltage curve increases with increase in load resistance and current decreases with increase in load resistance, as shown in Figure 3e. The output power is obtained using Equation $P = I^2R$, where I is the current value at external load resistance R. Initially, the output power is increased and reaches maximum at optimum load resistance and later decreases as external load resistance increases, as shown in Figure 3f. When the external load resistance matches the internal impedance of HT-TENG, the output power reaches a maximum value. The maximum peak power obtained is about 6.16 mW at an optimal load resistance of 45 MΩ, which is

sufficient to drive low-power-consumption electronics, proliferating application range of HT-TENG.

3.4. Performance of HT-TENG under the Influence of Humidity and Temperature and Applications

The effect on HT-TENG with varying humidity and temperature is studied. The experiment is carried out by placing the HT-TENG in a custom-made glovebox. By varying RH and temperature conditions, the influence of humidity and temperature on HT-TENG output performance was investigated. The majority of Earth's ambient areas have humidity and temperature ranges of 10 to 60%RH and 10 to 60 °C respectively. Also, as the EVA polymer reaches 60 °C, it loses its physical condition and becomes sticky, adhering to the PTFE top layer. This limits the contact and separation of top and bottom layers, which affects the device's performance. As a result, operating humidity and temperature are limited to 10 to 60%RH and 10 to 60 °C, respectively. The graphs of normalized voltage and normalized current

are plotted under varying RH ranging from 10% to 60%, as shown in **Figure 4**a,b, and temperature conditions ranging from 10 to 60 °C, as shown in Figure 4c,d.

The dielectric properties of the triboelectric materials, EVA,[23] and PTFE[24] are excellent. The dielectric constant of EVA and PTFE remains unchanged with the variation of temperature up to 70[23] and 250 °C[24] respectively. Furthermore, both polymers have a strong water resistance,[25] which prevents surface charge degradation Because of this uniformity, the output of HT-TENG stays stable and operating humidity and temperature are limited to 10 to 60%RH and 10 to 60 °C, which results in steady output performance under ambient environment conditions. A detailed material property of EVA and PTFE with respect to varying humidity and temperature is given in Note S3, Supporting Information. The output voltage and output current remained almost constant for varying humidity (Figure S3, S4,

Supporting Information) and temperature (Figure S5, S6, Supporting Information), which signifies that our HT-TENG produces stable output with varying humidity and temperature comparably better than other TENGs in **Table 1**.
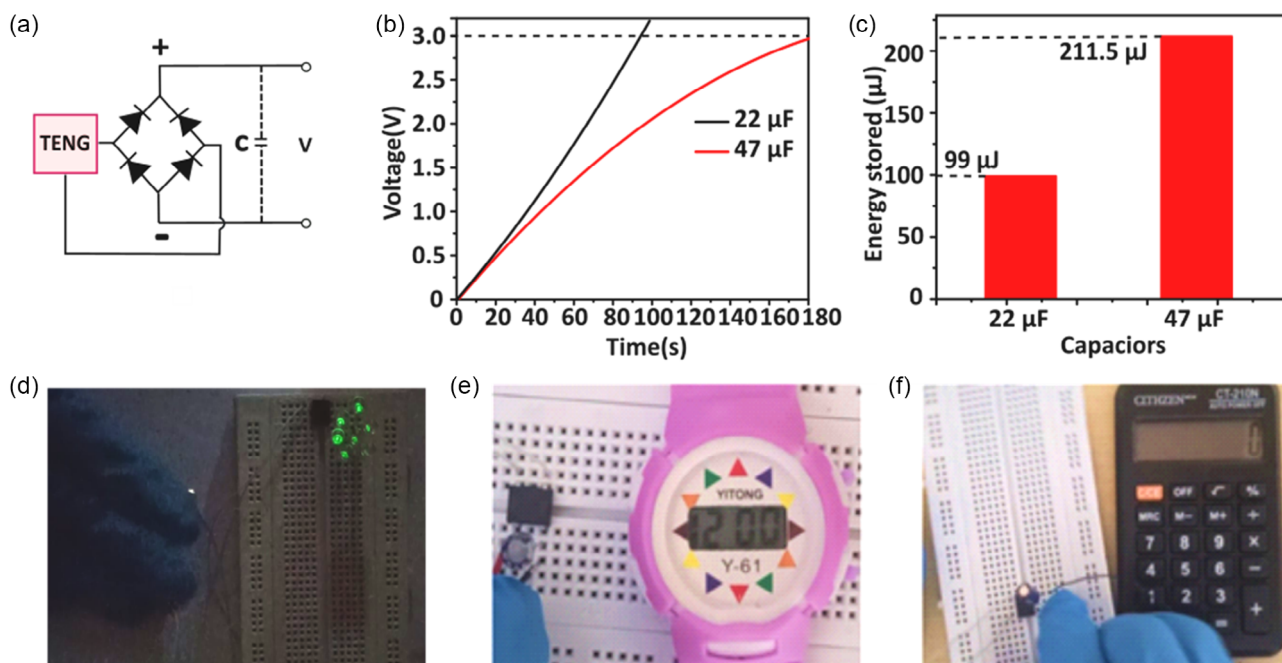
To validate the electrical output of the HT-TENG device, various confirmatory tests were performed, such as charging commercial capacitors, glowing green LEDs, powering up a digital wrist watch, and a calculator. The output power generated by the as-fabricated HT-TENG can be stored using a rectifier bridge in a capacitor, as shown in **Figure 5**a, which can be further used to power some electronic devices. Figure 5b reveals the charging curve of two commercial capacitors with the capacitance 22 and 47 µF, respectively, which are charged up to 3 V through a rectifier circuit. The 22 µF capacitor charged quickly to 3 V in 97.09 s, storing a maximum energy of 99 µJ. Similarly, 47 µF capacitor charged to 3 V in 180 s with the maximum energy storage of 211.5 µJ by gentle hand
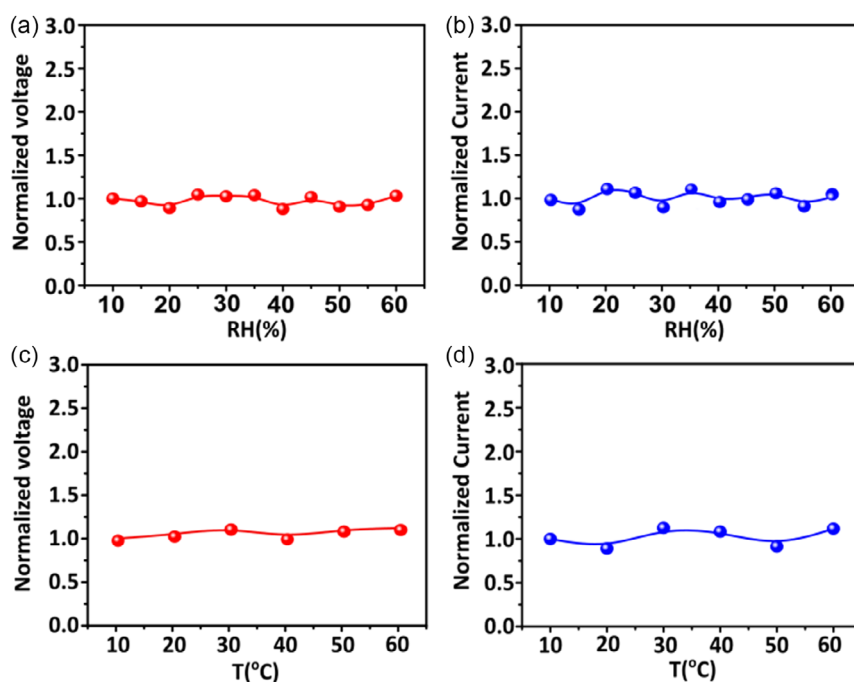
Figure 4. Humidity and temperature response of the HT-TENG. a) Normalized voltage and b) Normalized current of HT-TENG under various RH conditions ranging from 10 to 60%RH. c) Normalized voltage and d) normalized current of HT-TENG under various temperature conditions ranging from 10 to 60 °C.

Table 1. Comparison of output performance of other TENG devices with HT-TENG.

Trioactive materials	Humidity range	Temperature range	Output		Ref.
			Voltage [V]	Current [µA]	
PDMS and Al	10% to 90%		Decreases	–	[4b]
PTFE and fluorine-doped tin oxide glass	20% to 100%		Decreases	Decreases	[6]
Kapton and graphene oxide paper	20% to 99%		Decreases	Decreases	[26]
PTFE and PVDF		10 to 90 °C	Increases	–	[27]
PTFE and Al		−196 to 277 °C	Decreases	Decreases	[5b]
PTFE and Al		−20 to 150 °C	Decreases	–	[5c]
PTFE and EVA	10% to 60%	10 to 60 °C	Constant	Constant	Our work

ADVANCED SCIENCE NEWS
www.advancedsciencenews.com

pss rrl
physica status solidi
www.pss-rapid.com

Figure 5. Applications of HT-TENG a) TENG connected to a full-wave bridge rectifier circuit with capacitor. b) Commercial capacitors with 22 and 47 μF capacitance charged upto 3 V. c) Energy storage in the capacitors using the HT-TENG. d) Glowing green LEDs. Powering e) digital watch and f) calculator.

tapping, as shown in Figure 5c. The energy stored in a capacitor is calculated by the equation $E = CV^2/2$; detail calculations are given in Note S4, Supporting Information. The as fabricated HT-TENG is used to power green LEDs using a rectifier bridge (Figure 5d and Supporting Video S1, Supporting Information). The stored energy in a 22 μF capacitor with 3 V is utilized to power a digital wrist watch (Figure 5e and Supporting Video S2, Supporting Information) and a calculator (Figure 5f and Supporting Video S3, Supporting Information).

4. Conclusion

In summary, we report a HT-TENG, configured with contact and separation mode for effectively harvesting waste mechanical energy in to electricity. The as-fabricated HT-TENG generated a maximum peak of ≈210 V for the open-circuit voltage and the short- circuit current of ≈12.85 μA from hand-tapping energy. We have demonstrated that HT-TENG can efficiently work under various RH and temperature conditions ranging from 10 to 60%RH and temperature ranging from 10 to 60 °C respectively. Further, the output obtained is utilized for charging commercial capacitors with rectifying circuits, can power a series of green LEDs, digital wrist watches, and calculator. The proposed HT-TENG can be interfaced with portable/wearable electronic devices to work efficiently in ambient environment, thus showing the wide spectrum of applications and large-scale commercialization.

Supporting Information

Supporting Information is available from the Wiley Online Library or from the author.

Conflict of Interest

The authors declare no conflict of interest.

Data Availability Statement

The data that support the findings of this study are available from the corresponding author upon reasonable request.

[1] a) F.-R. Fan, Z.-Q. Tian, Z. L. Wang, *Nano Energy* **2012**, *1*, 328; b) J. Zhong, Q. Zhong, F. Fan, Y. Zhang, S. Wang, B. Hu,

ADVANCED
SCIENCE NEWS

www.advancedsciencenews.com

pss
physica status solidi rrl

www.pss-rapid.com

Z. L. Wang, J. Zhou, *Nano Energy* **2013**, *2*, 491; c) Y. Zhang, Z. Liu, D. Zang, Y. Qian, K. Lin, *Sci. China Phys. Mech. Astron.* **2013**, *56*, 1712; d) Z. L. Wang, L. Lin, J. Chen, S. Niu, Y. Zi, *Triboelectric Nanogenerators*, Springer, Berlin **2016**; e) S. A. Shankaregowda, C. B. Nanjegowda, X.-L. Cheng, M.-Y. Shi, Z.-F. Liu, H.-X. Zhang, *IEEE Trans. Nanotechnol.* **2016**, *15*, 435.

[2] a) S. Ankanahalli Shankaregowda, R. F. Sagade Muktar Ahmed, Y. Liu, C. Bananakere Nanjegowda, X. Cheng, S. Shivanna, S. Ramakrishna, Z. Yu, X. Zhang, K. Sannathammegowda, *Nanomaterials* **2019**, *9*, 1585; b) B. N. Chandrashekar, B. Deng, A. S. Smitha, Y. Chen, C. Tan, H. Zhang, H. Peng, Z. Liu, *Adv. Mater.* **2015**, *27*, 5210; c) B. N. Chandrashekar, A. S. Smitha, Y. Wu, N. Cai, Y. Li, Z. Huang, W. Wang, R. Shi, J. Wang, S. Liu, *Sci. Rep.* **2019**, *9*, 3999; d) S. A. Shankaregowda, R. F. S. M. Ahmed, C. B. Nanjegowda, J. Wang, S. Guan, M. Puttaswamy, A. Amini, Y. Zhang, D. Kong, K. Sannathammegowda, *Nano Energy* **2019**, *66*, 104141.

[3] a) S. Niu, S. Wang, L. Lin, Y. Liu, Y. S. Zhou, Y. Hu, Z. L. Wang, *Energy Environ. Sci.* **2013**, *6*, 3576; b) J. Shao, M. Willatzen, T. Jiang, W. Tang, X. Chen, J. Wang, Z. L. Wang, *Nano Energy* **2019**, *59*, 380; c) S. Chun, I. Y. Choi, W. Son, J. Jung, S. Lee, H. S. Kim, C. Pang, W. Park, J. K. Kim, *ACS Energy Lett.* **2019**, *4*, 1748.

[4] a) Z. Ren, Y. Ding, J. Nie, F. Wang, L. Xu, S. Lin, X. Chen, Z. L. Wang, *ACS Appl. Mater. Interfaces* **2019**, *11*, 6143; b) V. Nguyen, R. Yang, *Nano Energy* **2013**, *2*, 604; c) D. Jang, Y. Kim, T. Y. Kim, K. Koh, U. Jeong, J. Cho, *Nano Energy* **2016**, *20*, 283; d) R. Wen, J. Guo, A. Yu, J. Zhai, Z. L. Wang, *Adv. Funct. Mater.* **2019**, *29*, 1807655.

[5] a) K. Xia, Z. Zhu, H. Zhang, Z. Xu, *Appl. Phys. A* **2018**, *124*, 520; b) X. Wen, Y. Su, Y. Yang, H. Zhang, Z. L. Wang, *Nano Energy* **2014**, *4*, 150; c) C. X. Lu, C. B. Han, G. Q. Gu, J. Chen, Z. W. Yang, T. Jiang, C. He, Z. L. Wang, *Adv. Eng. Mater.* **2017**, *19*, 1700275.

[6] H. Guo, J. Chen, L. Tian, Q. Leng, Y. Xi, C. Hu, *ACS Appl. Mater. Interfaces* **2014**, *6*, 17184.

[7] H. Hwang, K. Y. Lee, D. Shin, J. Shin, S. Kim, W. Choi, *Appl. Surf. Sci.* **2018**, *442*, 693.

[8] C. Wu, A. C. Wang, W. Ding, H. Guo, Z. L. Wang, *Adv. Mater.* **2019**, *9*, 1802906.

[9] H. Zou, Y. Zhang, L. Guo, P. Wang, X. He, G. Dai, H. Zheng, C. Chen, A. C. Wang, C. Xu, *Nat. Commun.* **2019**, *10*.

[10] a) J. Chen, Z. L. Wang, *Joule* **2017**, *1*, 480; b) H. Ouyang, Z. Liu, N. Li, B. Shi, Y. Zou, F. Xie, Y. Ma, Z. Li, H. Li, Q. Zheng, *Nat. Commun.* **2019**, *10*; c) J. Wen, B. Chen, W. Tang, T. Jiang, L. Zhu, L. Xu, J. Chen, J. Shao, K. Han, W. Ma, *Adv. Energy Mater.* **2018**, *8*, 1801898.

[11] a) F. A. Hassani, C. Lee, *J. Microelectromech. Syst.* **2015**, *24*, 1338; b) S. W. Chen, X. Cao, N. Wang, L. Ma, H. R. Zhu, M. Willander, Y. Jie, Z. L. Wang, *Adv. Energy Mater.* **2017**, *7*, 1601255.

[12] a) Y. Li, J. Xiong, J. Lv, J. Chen, D. Gao, X. Zhang, P. S. Lee, *Nano Energy* **2020**, *78*, 105358; b) D. S. Kong, J. Y. Han, Y. J. Ko, S. H. Park, M. Lee, J. H. Jung, *Energies* **2021**, *14*, 1120.

[13] a) J. Reyes-Labarta, M. Olaya, A. Marcilla, *Polymer* **2006**, *47*, 8194; b) E. Dhanumalayan, G. M. Joshi, *Adv. Compos. Hybrid Mater.* **2018**, *1*, 247.

[14] a) T. Serafinavičius, J.-P. Lebet, C. Louter, T. Lenkimas, A. Kuranovas, *Procedia Eng.* **2013**, *57*, 996; b) H. Aglan, Y. Gan, M. El-Hadik, P. Faughnan, C. Bryan, *J. Mater. Sci.* **1999**, *34*, 83.

[15] a) X. Changlin, H. Junlin, H. Tao, C. Songmao, S. Jiarui, *Polym. Mater. Sci. Eng.* **1988**, *02*; b) W. Kan, H.-C. Li, J.-Y. Li, X.-J. Zhang, X.-F. Li, J.-D. Tang, W. Jing, L.-J. Wang, W. Ling, *Inte. Conf. on Applied Mechanics and Mechanical Automation*, AMMA **2017** ISBN: 978-1-60595-471-4.

[16] a) S. Xu, C. Zhou, J. Li, L. Shen, H. Lin, *Mater. Today Commun.* **2021**, *26*, 102114; b) H. Kim, J. Jang, S. Sohn, *J. Korean Phys. Soc* **2010**, *5*, 1281.

[17] T. Kumar, B. Pandey, T. Das, D. A. Hussain, presented at *2014 6th Int. Congress on Ultra Modern Telecommunications and Control Systems and Workshops (ICUMT)*, St. Petersburg, Russia **2014**.

[18] F. Pern, A. Czanderna, *Sol. Energy Mater. Sol. Cells* **1992**, *25*, 3.

[19] Z. Xia, R. Gerhard-Multhaupt, W. Künstler, A. Wedel, R. Danz, *J. Phys. D: Appl. Phys.* **1999**, *32*, L83.

[20] a) Q. Li, L. M. Matuana, *J. Appl. Polym. Sci.* **2003**, *88*, 3139; b) A. K. Bledzki, O. Faruk, *Compos. Part A* **2006**, *37*, 1358.

[21] M. A. Jacobs, M. F. Kemmere, J. T. Keurentjes, *Polymer* **2004**, *45*, 7539.

[22] D. Kim, S. Lee, Y. Ko, C. H. Kwon, J. Cho, *Nano Energy* **2018**, *44*, 228.

[23] K. Agroui, B. Koll, G. Collins, M. Salama, A. H. Arab, A. Belghachi, N. Doulache, M. Khemici, presented at *Reliability of Photovoltaic Cells, Modules, Components, and Systems*, San Diego, California, United States **2008**.

[24] K. Murali, S. Rajesh, K. S. Jacob, O. Prakash, A. Kulkarni, R. Ratheesh, *J. Mater. Sci. Mater. Electron.* **2010**, *21*, 192.

[25] a) K. Wu, Z. Wang, *Polymer* **2008**, *47*, 247; b) K. L. Campbell, M. A. Sidebottom, C. C. Atkinson, T. F. Babuska, C. A. Kolanovic, B. J. Boulden, C. P. Junk, B. A. Krick, *Macromolecules* **2019**, *52*, 5268.

[26] F. Ejehi, R. Mohammadpour, E. Asadian, S. Fardindoost, P. Sasanpour, *Microchim. Acta* **2021**, *188*, 251.

[27] K. Xia, Z. Zhu, H. Zhang, Z. Xu, *Appl. Phys. A* **2018**, *124*, 520.